CHEMICAL ENGINEERING TRANSACTIONS
VOL. 117, 2025
A publication of AIDIC
The Italian Association of Chemical Engineering
Online at www.cetjournal.it
Guest Editors: Fabrizio Bezzo, Flavio Manenti, Gabriele Pannocchia, Almerinda di Benedetto

ISBN 979-12-81206-17-5; **ISSN** 2283-9216
DOI: 10.3303/CET25117133

The Impact of Powder Delivery Process Parameters on Spreading Behaviour in Powder Bed Fusion Additive Manufacturing

Bruno Nicola Dose[a,*], Sina Zinatlou Ajabshir[a], Ali Hassanpour[b], Diego Barletta[a], Massimo Poletto[a]

[a] Department of Industrial Engineering, University of Salerno – Via Giovanni Paolo II, 132 – 84084 Fisciano (SA), Italy
[b] Department of Chemical and Process Engineering, University of Leeds – LS29JT, UK
bdose@unisa.it

In this study, the effects of spreading speed and bed temperature on powder spreading in the Laser-Beam Powder Bed Fusion (PBF-LB) process were investigated. A purposely developed image analysis method was used to evaluate powder spread quality. High-resolution macro images covering most of the powder layer (10×7 cm) were captured and processed to obtain a wavelet power spectrum to highlight the distribution of roughness wavelengths on the layer surface. Results showed that increasing spreading speed and bed temperature widened the spectral density distribution of roughness wavelengths. The Spreadability Index (SI), defined as the ratio of the median particle size to the dominant surface wavelength, decreased by 7% when the temperature rose from 25 °C to 80 °C at a spreading speed of 3 mm/s. At a constant temperature of 25 °C, increasing the spreading speed from 3 mm/s to 30 mm/s reduced the SI by 64%, highlighting the significant impact of spreading speed on powder quality.

1. Introduction

Additive manufacturing (AM) revolutionizes production by building items layer by layer from digital models. It minimizes material waste and enables complex geometries unattainable with subtractive methods (Gopal et al., 2022). Furthermore, the fewer geometrical constraints in AM foster innovative design without additional costs, enhancing efficiency and creativity in product development (Hitzler et al., 2018). Laser-Beam Powder Bed Fusion (PBF-LB), a key AM technique, includes Selective Laser Melting (SLM) and Selective Laser Sintering (SLS). SLM fully melts powder for dense, strong parts, while SLS partially fuses particles, forming solid bonds (Zohdi and Yang, 2021).

Regardless of the method, it was demonstrated that in PBF, the quality of each powder layer obtained by the spreading process can affect the overall quality of the final product (Boschetto et al., 2024; Horn et al., 2024). In the attempt to correlate powder spreadability to its flowability (Salehi et al., 2022; Yim et al., 2022a), it was demonstrated that powders showing similar flowing behaviour can be characterized by a completely differen spreading behaviour (Guo and Moudgil, 2024; Mehrabi et al., 2023; Nan and Gu, 2022; Vakifahmetoglu et alt, 2021; Yim et al., 2022b). Consequently, the characterization of powder spreadability requires dedicated experimental equipment and procedures able to reproduce stresses, temperatures and movement conditions in commercial machines. A standardized procedure and metric to quantify spreadability have not been established yet, and different methods account for powder bed surface roughness and density.

In PBF techniques, each spread layer affects final product quality. Layer defects may accumulate, compromising geometry and mechanical properties (Boschetto et al., 2024). However, evident defects in the layer are not the only factors that may contribute to inferior product properties. Consequently, various techniques and procedures are currently employed to evaluate the characteristics of the layers. These techniques can be categorized into three main types of analysis: defect-based, density-based, and surface-based.

Defect-based methods may include the assessment of powder layer defects and defects in the final product. Evaluating flaws in the final product avoids directly monitoring powder behaviour during spreading and returns valuable information on some external parameters. For instance, Horn et al. (2024) demonstrated the impact of

Paper Received: 15 December 2024; Revised: 5 February 2025; Accepted: 26 May 2025
Please cite this article as: Dose B.N., Zinatlou Ajabshir S., Hassanpour A., Barletta D., Poletto M., 2025, The Impact of Powder Delivery Process Parameters on Spreading Behaviour in Powder Bed Fusion Additive Manufacturing, Chemical Engineering Transactions, 117, 793-798 DOI:10.3303/CET25117133

using different spreading tools for PBF with a metal powder (Inconel®), assessing the geometrical and physical properties of the final artefact. Building artefacts with different shapes, dimensions and angles, this study highlights that different spreading tools offer distinct advantages and disadvantages, largely due to their stiffness and the normal pressure applied to the powder layer (Horn et al., 2024). Boschetto et al. (2024) focused more closely on flaws present in individual layers, demonstrating that some defects accumulate throughout the process while others either disappear in subsequent layers or remain outside the processed area, thus becoming non-influential to product quality. Building on this approach, Rüther et al. (2023) developed a procedure to identify flaws in the powder layer and associate a severity score based on the depth and position of each flaw. Density-based methods assess the packing density of the powder layer relative to the powder used. Different methods may refer to different layer volumes. Brika and Brailovski (2023) proposed a correction to account for the powder loss through tray gaps during spreading. One of the most common approaches is to define the layer's height using the d_{90} of the powder (Nan and Gu, 2022), assuming it represents the minimum expected width of the band, including height variation over the surface of a powder bed made of loose particles. Surface-based methods evaluate powder layer quality using non-contact techniques like confocal microscopy (Tang et al., 2023), X-ray imaging (Penny et al., 2021), or image analysis. Confocal microscopy and X-ray methods for surface quality assessment face limitations due to their ex-situ nature, requiring powder bed relocation and restricting analysis to small areas. Using grazing light to enhance contrast, image analysis techniques capture greyscale images processed pixel by pixel. A common approach involves binarizing the image by selecting an appropriate threshold to highlight visible defects or uncovered areas. The results are typically presented as the ratio of the defect area to the total area (Vakifahmetoglu et al., 2021). Another widely used technique evaluates shadows created by grazing light over the layer's surface, analysing pixel intensity along a straight line in the spreading direction. This method is more suitable when there are no evident flaws. The pixel intensity signal can be further processed using wavelet transforms (Zinatlou Ajabshir et al., 2024b) or Fourier transforms (Salehi et al., 2022). Wavelet analysis can better describe non-periodical signals, which leads to higher frequency accuracy than Fourier analysis (Cao et al., 2023). Recent approaches have also explored correlations between pixel intensity and powder bed roughness. However, these techniques remain under development, with ongoing efforts focused on defining reference heights and understanding the dependence of pixel intensity on light source parameters.

This work includes the most recent improvements in the development of a new characterization procedure employing image analysis on a polymeric powder layer and in the design of a novel spreading apparatus, improving the spreading device and the surface analysis procedures developed at the University of Salerno ((Lupo et al., 2023; Zinatlou Ajabshir et al., 2024b).

2. Experimental setup, materials and procedures

2.1 Setup and image acquisition procedure

Spreading tests were conducted at different temperatures and spreading speed conditions. These experiments utilised the spreading apparatus at the University of Salerno (Sofia et al., 2019). This setup allows for assessing the behaviour of various powders and investigating the fundamental mechanisms underlying the spreading process (Lupo et al., 2023; Zinatlou Ajabshir et al., 2024b). Introducing radiative heating sources and improving the chamber insulation, the modified setup (Figure 1a) reached a maximum spreading temperature of approximately 200°C. This temperature corresponds to an 80°C increase in the maximum temperature achievable in the experiments. In previous experiments, the image of the powder bed was acquired using the combination of a camera and a microscope. While this setup offered high resolution, it was limited to capturing images with dimensions of up to 1 mm, representing just 1/100th of the total powder bed area. To address this limitation, adjacent images were taken, increasing the coverage in the spreading direction to a maximum of 1 cm. This process was time-intensive, requiring significant efforts for both acquisition and post-processing to merge the images into a single stripe. Therefore, it was impractical to produce larger images. Consequently, the power spectra obtained had a small statistical base, affected by important fluctuations and relevant to only a small portion of the bed. To overcome these limits, the new image acquisition system employs a high-resolution camera to ensure efficient pixel representation of particles while enabling the capture of the entire powder bed dimension in the spreading direction in a single image. The camera is positioned on a tripod to reach the right image acquisition condition. The system is complemented by a LED lamp flushing grazing light on the powder layer at 45° (Figure 1b).

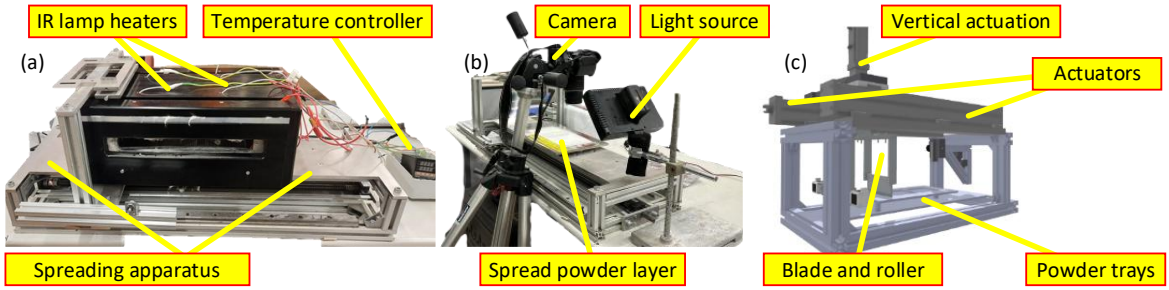

Figure 1 Experimental setup: a) Set up used in the experiment with an improved heating system; b) image acquisition setup for high-resolution images of the powder bed c) set up designed on the experience gained in this and previous studies.

The Fujifilm XT5 (40 MP) and 60 mm macro lens were chosen for optimal field of view and resolution, ensuring precise particle representation.

2.2 Materials and methods

To ensure consistency in the analysis, the polymeric powder and the testing conditions were kept identical to those used in the test conducted with a microscopic camera for image analysis (Zinatlou Ajabshir et al., 2024b). The tests were conducted on polyamide PA6, a polymeric powder developed by SINTERLINE® for PBF. Table 1 provides the relevant powder properties.

Table 1: Characteristics of PA6 powder, $T_{melting}$ *denotes the melting point of the polymer,* ρ_B *and* ρ_P *represent bulk and particle density, respectively,* d_x *corresponds to the diameter of the* x^{th} *percentile of the particle size distribution,* $d_{3,2}$ *is the Sauter diameter,* $d_{4,3}$ *is the volume-weighted diameter, span is defined as* $(d_{90} - d_{10})/d_{50}$ *while* SSA *is the specific surface area.*

$T_{melting}$ [°C]	ρ_B [kg/m³]	ρ_P [kg/m³]	d_{10} [µm]	d_{50} [µm]	d_{90} [µm]	$d_{3,2}$ [µm]	$d_{4,3}$ [µm]	span	SSA [m²/g]
210	525	1130	15	46	91	20	50	1.65	0.303

Layer images were captured with the camera positioned above the powder bed at approximately 170 mm, measured from the layer surface to the camera's sensor with the longer side of the image in the spreading direction. This positioning provided an image of 7×10 cm of the powder bed and was selected to maximize the number of pixels per particle in this direction. The rectangular shape of the image leaves out two 1.5 cm bands from the sides of the powder bed. Assuming spherical particles and using the d_{50} as a reference, this setup ensures a resolution of 3 pixels per particle diameter in the spreading direction, a value that is comparable to the resolution achieved with the previous microscopic imaging setup. Constant light conditions were maintained using a 45° grazing light. Tests were performed on the spreading apparatus at two temperatures, 25°C and 80°C, and two spreading speeds, 3 mm/s and 30 mm/s, to assess the capability of the acquisition method to produce reliable results. Before each test, the powder was dried at 110°C for 24 hours and then cooled in a desiccator with silica beads for 1.5 hours to prevent moisture absorption. The improved heating system enabled the apparatus to reach 80°C within approximately 5 minutes, after which the temperature was maintained for 1 hour to ensure uniformity. The captured images were processed with image analysis, dividing the image into 1288 stripes along the spreading direction, and the most significant wavelengths of each stripe were identified using a wavelet transform processed using a Matlab Tool. These wavelengths were then averaged to produce a single power spectrum representing the surface quality of the powder layer. The peak length of the average power spectrum was used to calculate the Spreadability Index (SI), providing a quantitative measure of layer quality.

3. Results

Figure 2 shows macro images of the powder bed under different conditions and the wavelet power spectra. Due to the larger basis of the image analysis possible with the high-resolution imaging of the layer, the quality of the power spectra obtained with the new technique appears much better than the one provided previously by (Zinatlou Ajabshir et al., 2024b) . Images qualitatively show the appearance of a macroscopic wavy surface at higher spreading speeds, quantitatively confirmed by a shift of the maxima of power spectra towards higher wavelength (Figures 2b and 2d). Also, temperature produces a worsening of the surface, which is visible as more marked surface waves and more consistent contributions of the millimetric wavelengths in the power

spectra (Figures 2c and 2d). Key parameters were extracted to represent surface roughness distribution, including the most predominant wavelength (peak length, pl) and 60% of the pl at both ends (shorter wavelength, *swl*, and larger wavelength, *lwl*).

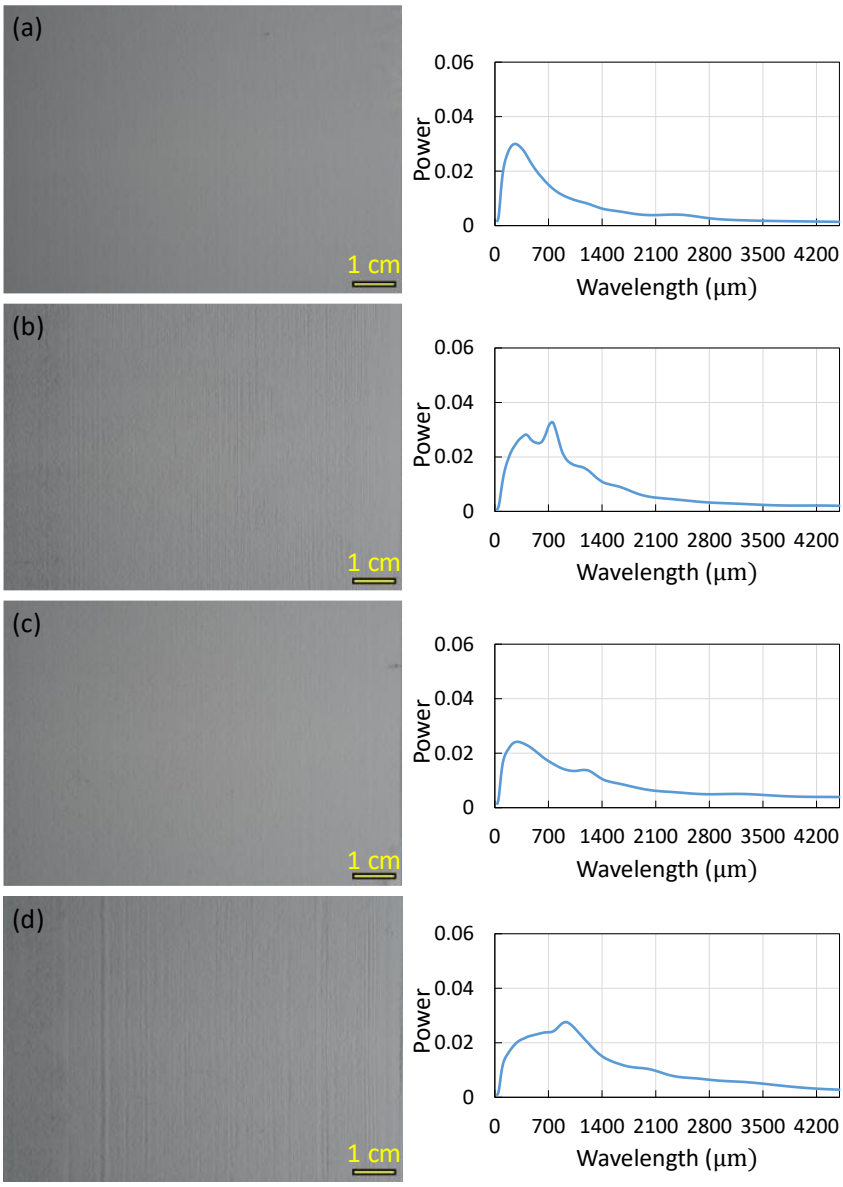

Figure 2: Captured image and power spectrum of PA6 at: a) 3 mm/s and 25°C; b) 30 mm/s and 25°C; c) 3 mm/s and 80°C; d) 30 mm/s and 80°C.

Figure 3 displays some of the key parameters of the surface roughness distribution, identified as the wavelet corresponding to the peak of the powder spectrum distribution and, respectively, the minimum and the maximum wavelength at which the power spectrum attains a value equal to 60% of the original.

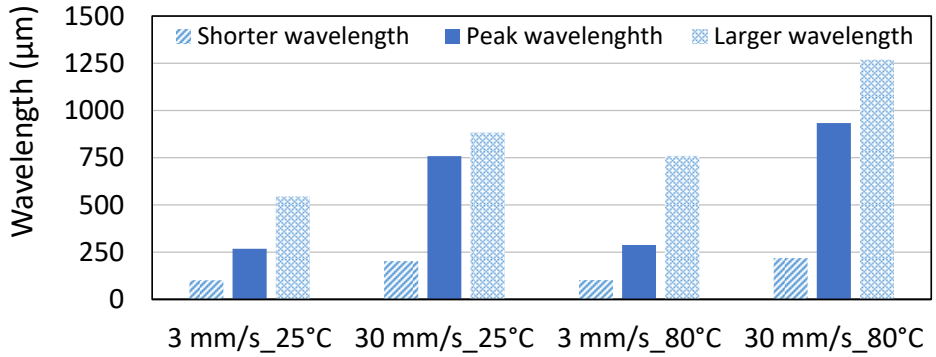

Figure 3: Characteristic wavelengths of the surface roughness distribution at various spreading conditions.

Powders tend to settle in piles characterized by similar profile angles. It is assumed, therefore, that lower wavelengths should also correspond to lower roughness profiles. Lower peak length values (pl) should correspond to smother surfaces, hence the definition of the Spreadability Index (Zinatlou Ajabshir et al., 2024a) can be presented as follows:

$$Spreadability\ Index\ (SI) = \frac{d_{50}}{pl} \quad (1)$$

Where d_{50} and pl are the median particle size and peak length, respectively. Higher Spreadability Indexes would mean smaller peak length per median particle size, hence should correspond to a higher quality of the layer surface. The values of the Spreadability Index (SI) results displayed in Figures 4 confirm the expected trends of negative effects of the spreading speed and temperature.

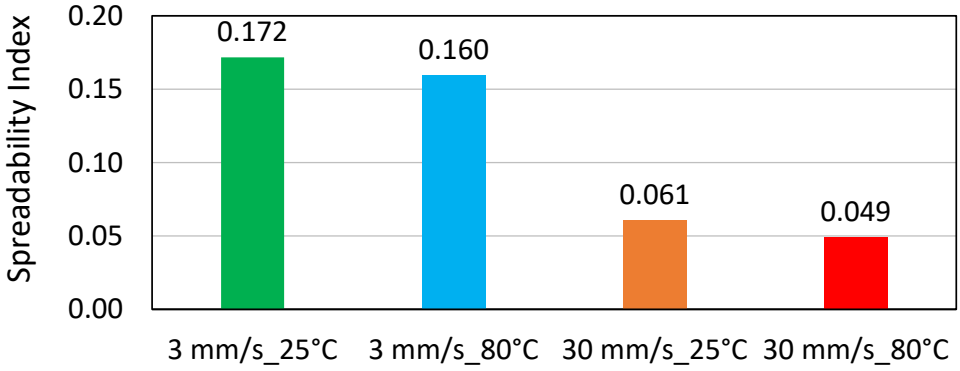

Figure 4: Spreadability Index of PA6 at different testing conditions.

A possible factor contributing to the appearance of the visible and rather periodic waves at the highest spreading speed, as shown in Figure 2, might be the vibrations of the rails on which the trailer holding the blade moves. To avoid these testing artefacts and overcome other experimental limitations of the existing setup, a new setup has been designed for use in the next research steps.

3.1 Proposed experimental setup

The experimental setup, represented in Figure 1c, has been re-designed to adjust the blade position precisely despite temperature effects and to reach higher spreading speeds. The design ensures higher reliability by producing results under conditions closely resembling those of commercial equipment while retaining the possibility to explore a wide range of spreading speeds and temperatures. The spreading setup consists of two actuators and a guide to provide biaxial motion of the spreading tool, enabling vertical and horizontal movement automation. The frame hosting the spreading tools is designed to simultaneously accommodate both a blade and a roller, facilitating combined tests in future studies. The actuator responsible for motion in the spreading direction, defined as the y-axis, enables horizontal movement of the blade at speeds up to 300 mm/s, comparable to the typical spreading speeds of commercial machines. The vertical actuator enables multilayer testing and adjustment of the spreading tool (a blade-shaped recoater) by allowing fine vertical positioning during high-temperature tests, thus mitigating the effects of thermal expansion on the blade and its holder. Additionally, the actuators and guide are positioned above the spreading plate to minimise the risk of fouling.

4. Conclusions

A new image acquisition procedure and an improved heated chamber were developed to extend the ability of the experimental apparatus previously developed at the University of Salerno to spread powder layers and study their quality. A high-resolution camera is used for the image acquisition procedure. Tests with the new procedure enabled the analysis of the entire powder bed length in the spreading direction, providing a more comprehensive and reliable layer characterisation. The results, representing nearly the whole layer, demonstrate significantly reduced noise, as evidenced by the smoother power spectra. The findings in the system testing experiments are consistent with expectations, confirming that higher spreading speeds and temperatures degrade the quality of the spread layer. The variations in the SI indicated that the powder is more sensitive to changes in spreading speed than to variations in temperature within the tested range. These tests validate the effectiveness of the new acquisition technique and heated chamber in advancing the understanding and optimisation of the spreading process. Some shortcomings of the existing setup will be overcome in a new apparatus purposely designed. This setup will also address vibrational issues identified during testing while.

Acknowledgements:

This work was supported by the University of Leeds Impact Acceleration Account (grant reference: EP/X52573X/1).

References

Boschetto, A., Bottini, L., Vatanparast, S., 2024. Powder bed monitoring via digital image analysis in additive manufacturing. J Intell Manuf 35, 991–1011.

Brika, S.E., Brailovski, V., 2023. A Novel Apparatus for the Simulation of Powder Spreading Procedures in Powder-Bed-Based Additive Manufacturing Processes: Design, Calibration, and Case Study. Journal of Manufacturing and Materials Processing 7, 135.

Cao, X., Shi, J., Zhang, C., Zheng, J., 2023. Inter-comparison of wave skewness and asymmetry estimation using wavelet, Fourier and statistical methods. Ocean Engineering 268, 113382.

Horn, M., Schmitt, M., Langer, L., Schlick, G., Seidel, C., 2024. Laser powder bed fusion recoater selection guide—Comparison of resulting powder bed properties and part quality. Powder Technol 434, 119356.

Lupo, M., Zinatlou Ajabshir, S., Sofia, D., Barletta, D., Poletto, M., 2023. Experimental metrics of the powder layer quality in the Selective Laser Sintering process. Powder Technol 419, 118346.

Nan, W., Gu, Y., 2022. Experimental investigation on the spreadability of cohesive and frictional powder. Advanced Powder Technology 33, 103466.

Penny, R.W., Praegla, P.M., Ochsenius, M., Oropeza, D., Weissbach, R., Meier, C., Wall, W.A., Hart, A.J., 2021. Spatial mapping of powder layer density for metal additive manufacturing via transmission X-ray imaging. Addit Manuf 46, 102197.

Rüther, M., Klippstein, S.H., Ponusamy, S., Rüther, T., Schmid, H.-J., 2023. Flowability of polymer powders at elevated temperatures for additive manufacturing. Powder Technol 422, 118460.

Salehi, H., Cummins, J., Gallino, E., Harrison, N., Hassanpour, A., Bradley, M., 2022. A new approach to quantify powder's bed surface roughness in additive manufacturing. Powder Technol 407, 117614.

Sofia, D., Lupo, M., Barletta, D., Poletto, M., 2019. Validation of an Experimental Procedure to Quantify The Effects of Powder Spreadability on Selective Laser Sintering Process. Chem Eng Trans 74, 397–402.

Tang, M., Guo, Y., Zhang, W., Ma, H., Yang, L., Wei, W., Wang, L., Fan, S., Zhang, Q., 2023. On recoated powder quality with a forward rotating flexible roller in laser powder bed fusion of 30 wt% 5 μm SiCp/AlSi10Mg composites. Mater Des 225, 111489.

Vakifahmetoglu, C., Hasdemir, B., Biasetto, L., 2021. Spreadability of Metal Powders for Laser-Powder Bed Fusion via Simple Image Processing Steps. Materials 15, 205.

Zinatlou Ajabshir, S., Hare, C., Sofia, D., Barletta, D., Poletto, M., 2024a. Investigating the effect of temperature on powder spreading behaviour in powder bed fusion additive manufacturing process by Discrete Element Method. Powder Technol 436, 119468.

Zinatlou Ajabshir, S., Sofia, D., Hare, C., Barletta, D., Poletto, M., 2024b. Experimental characterisation of the spreading of polymeric powders in powder bed fusion additive manufacturing process at changing temperature conditions. Advanced Powder Technology 35, 104412.